# Single-Molecule Enzymology of Chymotrypsin Using Water-in-Oil Emulsion

Alan I. Lee and James P. Brody
Department of Biomedical Engineering, Henry Samueli School of Engineering, University of California, Irvine, California

ABSTRACT Single-molecule studies allow the study of subtle activity differences due to local folding in proteins, but are time consuming and difficult because only a few molecules are observed in one experiment. We developed an assay where we can simultaneously measure the activity of hundreds of individual molecules. The assay utilizes a synthetic chymotrypsin substrate that is nonfluorescent before cleavage by chymotrypsin, but is intensely fluorescent afterward. We encapsulated the enzyme and substrate in micron-sized droplets of water surrounded by silicone oil where each microdroplet contains $<1$ enzyme on average. A microscope and charge-coupled device camera are used to measure the fluorescence intensity of the same individual droplet over time. Based on these measurements, we conclude that enzymatic reactions could occur within this emulsion system, the statistical average activity of individual chymotrypsin molecules is similar to that measured in bulk, and the activity of individual chymotrypsin is heterogeneous.

## INTRODUCTION

The structure or conformation of a protein determines its function. A protein's chain of amino acids can exist in a large number of similar conformations, or substates. (Engler et al., 2003; Frauenfelder et al., 2003). In a population of proteins, each with an identical amino acid sequence, every protein could be folded into a slightly different structural substate. Therefore, each protein might exhibit slightly differing function or activity (Lu et al., 1998; Nie and Zare, 1997; Xie and Lu, 1999). Enzymes are a class of proteins where the function can be measured as chemical activity. By monitoring the activity of a collection of individual enzymes, one can better understand the different structural substates in which each enzyme can exist.

The technique of single-molecule detection can provide two types of information on protein activity. The first is detailed timing of the activity, and the second is a measure of the statistical distribution of the activity. Most single-molecule experiments focus on measuring the time evolution of the individual molecule's activity. This provides a detailed picture of the dynamic conformation of the molecule. However, this observation does not make the connection from the individual molecules to the ensemble averages that classical experiments observe. The statistical study of a population of single molecules provides the missing link. With both forms of information, one can discern molecular behavior that is otherwise hidden within the ensemble average (Edman et al., 1999; Ishii et al., 2003; Ishijima and Yanagida, 2001; Lu et al., 1998; Medina and Schwille, 2002; Xie and Lu, 1999; Xie and Trautman, 1998).

Experiments based on single-molecule detection have contributed to models of molecular motor dynamics, protein folding dynamics, and enzyme kinetics. Now instead of computer simulation, researchers can visualize how a molecular motor moves, as in the studies of myosin and F1-ATPase motor (Ishii et al., 2003; Ishii and Yanagida, 2000; Ishijima et al., 1991; Noji et al., 1997). Instead of speculating on how a protein structure changes during a reaction process, the structural changes can be monitored (Weiss, 1999; Weiss, 2000; Yang et al., 2003). Enzyme kinetics is no longer limited to the analysis of various ensemble constants. The fundamental characteristics of the enzyme can be analyzed using single-molecule detection (Edman et al., 1999; Edman and Rigler, 2000; Qian and Elson, 2002). Many different techniques for single-molecule detection exist, each with unique characteristics. These techniques monitor electrical, physical, or optical changes. The measurements for electrical and physical changes require physical contact with the molecule of interest (Allen et al., 2003; Edwardson and Henderson, 2004; Ha, 2001; Hinterdorfer et al., 2001; Ishii et al., 2003; Ishii and Yanagida, 2000; Kulzer and Orrit, 2004; Liem et al., 1995; Muller et al., 2002; Park et al., 2002; Sakmann and Neher, 1984). Measurements in optical changes allow the researcher to visually locate the molecule for study through noninvasive methods and observe the function of the molecule in its natural environment (Ha, 2001; Ishii et al., 2003; Ishii and Yanagida, 2000; Jares-Erijman and Jovin, 2003; Kulzer and Orrit, 2004; Medina and Schwille, 2002).

A persistent problem with single-molecule studies of proteins is the lack of statistics. We sought a method to measure the activity of hundreds of proteins individually, yet simultaneously. This would enable one to sample a statistically significant number of proteins and quantify the diversity of molecular activities.

*Submitted October 26, 2004, and accepted for publication March 1, 2005.*

Address reprint requests to James P. Brody, Dept. of Biomedical Engineering, Henry Samueli School of Engineering, University of California, Irvine, CA 92697. E-mail: jpbrody@uci.edu.



0006-3495/05/06/4303/09 $2.00

doi: 10.1529/biophysj.104.055053

We developed an assay for chymotrypsin, a well-studied model protease. The assay uses a profluorescent substrate that becomes fluorescent after cleavage, an optical detection system based on a charge-coupled device (CCD) camera that has thousands of optical detectors (pixels) in parallel, and a water-in-oil emulsion that, in essence, provides individual nanoscale test tubes for the chymotrypsin molecules.

## METHODS

### Microscope/CCD description

The microscope we used in this experiment is a Nikon (Tokyo, Japan) Eclipse TE200 inverted microscope with an attached 100W mercury lamp. The excitation light and the emission fluorescence are filtered through a Chroma (McHenry, IL) HQ FITC filter block set (excitation 480/40 nm, emission 535/50 nm). The objective is a 40× oil immersion Nikon Plan Fluor objective lens, with a numerical aperture of 1.30. The CCD camera we used in this experiment is a 12-bit Apogee 7p air-cooled CCD camera. The CCD camera is cooled down to −20°C for image acquisition. The CCD camera employs a SITe 512 × 512 back-illuminated CCD chip. The chip has a quantum efficiency of 75% at 520 nm.

### Emulsion generation

The water-in-oil emulsion is generated by placing ~10 mL of silicone oil (Fisher Scientific, Hanover Park, IL), 100 $\mu$L of 0.76 nM $\alpha$-chymotrypsin solution (Sigma Chemical, St. Louis, MO), and 100 $\mu$L of 150 $\mu$M substrate, Suc-$(AAPF)_2$-R110 (Molecular Probes, Eugene, OR), both in 10 mM HEPES buffer, pH 7.0, inside the miniblender for a Waring blender. This results in 0.38 nM $\alpha$-chymotrypsin and 75 $\mu$M substrate as the final concentration within the water phase. The enzyme molecule/substrate molecule ratio is ~1:200,000 in a 1-$\mu$m-diameter droplet, ensuring that the enzyme will be operating at the maximum velocity. The blender runs at 20,000 RPM for 30 s; ~800 $\mu$L of the resulting emulsion is taken and centrifuged at 6000 rpm for 30 s to sediment the larger droplets, allowing a more uniform droplet size distribution for loading.

### Control experiments

The positive control experiment is performed by generating an emulsion containing 200 $\mu$L 10 $\mu$M of R110 standard (Molecular Probes) in 10 mM HEPES buffer and loading the emulsion into the microfluidic device for observation under a 40× objective lens. The fluorescence resulting from the R110 standard is recorded by the CCD camera, with the same interval and exposure time as in the experimental setup. A negative control is also performed by replacing the R110 standard with 100 $\mu$L of 150 $\mu$M substrate and 100 $\mu$L of 10 mM HEPES buffer.

### Chymotrypsin assay

Chymotrypsin is a protease. It preferentially hydrolyzes peptide bonds involving tyrosine, phenylalanine, and tryptophan. We obtained chymotrypsin from Sigma Chemical, where it is purified from bovine pancreas. Its activity can be measured using the profluorescent substrate AAPF (Molecular Probes) which becomes fluorescent (excitation 492 nm/emission 521 nm) when cleaved by chymotrypsin.

The bulk chymotrypsin assay is done in a 96-well plate using a fluorescence reader (Fluoroskan Ascent FL, Thermo Labsystems, Altrincham, UK). One hundred microliters of 0.76 nM $\alpha$-chymotrypsin solution and 100 $\mu$L of 150 $\mu$M substrate, both in 10 mM HEPES buffer, are mixed together, which results in the same final concentration as in the single-molecule experiment. This will guarantee that the kinetics observed with the bulk population can be used for comparison to the single-molecule experiment because both have the same enzyme/substrate ratio (1:200,000). The enzymatic reaction is observed for 3 h at 1-min intervals. The fluorescence is collected with a 1-s exposure with a filter pair of 485 nm/527 nm.

The single-molecule chymotrypsin assay is performed by loading the emulsion into a grid-like polydimethylsiloxane microfluidic device (Whitesides et al., 2001) bonded to a glass coverslip, which provides a chamber with a dimension of 200 × 200 × 35 $\mu$m. The droplets inside the microfluidic device are fairly immobilized in all directions. Any minor fluctuation in the *x-y* direction can be realigned using software. The emulsion is observed under a 40× objective lens. The fluorescence resulting from the enzymatic reaction is recorded by a CCD camera, with an interval of 8 min and an exposure time of 500 ms. The starting time is established with the first CCD image. This is typically 5–10 min after mixing. We choose the first image for the starting time to avoid the problem of establishing how much fluorophore is being produced between the start of the mixing and the first image. With starting time set at the first image, we can ignore the fluorophore produced before and start with a new baseline.

### Image processing/tracking

The fluorescence image is taken with the software provided by the manufacturer of the CCD camera, MaxIm DL version 2.12. The raw image is calibrated to correct for intrinsic camera bias, dark noise, and uneven lighting due to optics. The calibrated images are loaded into image analysis software, MetaMorph 6.0. The droplets are tracked over time with the integrated morphology analysis function in MetaMorph 6.0. The images are stacked in chronological order and the droplets are aligned to the same position. A filtering rule is set to filter droplet size based on the pixel area (<15 pixels) covered by the fluorescent spot. Any spots >1 $\mu$m in diameter are discarded by the software. The position and fluorescence intensity are recorded in Microsoft Excel spreadsheets. The droplet data is then screened where droplets with high background noise are excluded and finally sorted to match droplets at different time points using droplet position with a simple algorithm written in LabView 6.0. Any droplet that is not present at all time points is dropped out. The droplet fluorescence is then scaled against the bulk data for easier comparison.

### Normalization to reference standards

The optical system has intrinsic variations of ~10–12%. To reduce these random fluctuations, red fluorescent microspheres (I-7224, Molecular Probes) with an emission spectrum similar to Texas Red are employed. The microspheres are 2.5 $\mu$m in diameter, and were purchased suspended in aqueous buffer. We evaporated the aqueous buffer from the microspheres and resuspended the microspheres inside silicone oil. This allows the fluorescent microspheres to behave like the aqueous droplets in the emulsion. Ten microliters of the microspheres solution is mixed in with 40 $\mu$L of centrifuged emulsion and loaded into the microfluidic device. The fluorescence from the microspheres is recorded and tracked using the same method for tracking droplets over time. The final processed data for individual microspheres are averaged, and this averaged value is used as the basis for normalization of intrinsic optical variations.

## RESULTS

We are confident that we are measuring the activity of an individual enzyme molecule 90% of the time. The distribution of enzymes within droplets is random and thus follows the Poisson distribution (see Fig. 1). Using this distribution, we calculate that at a working concentration of 0.38 nM (equivalent to a mean concentration of 0.12 molecules/1-$\mu$m-diameter

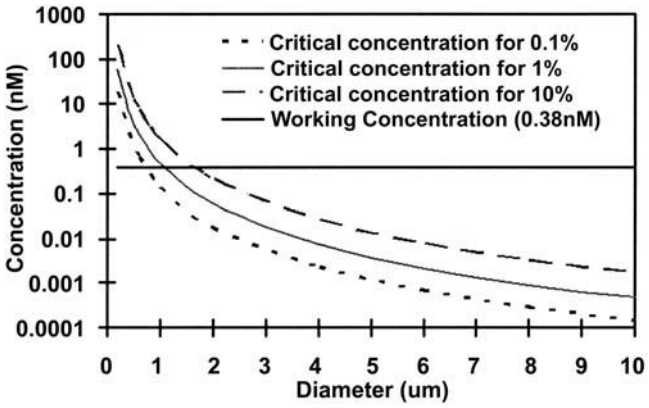


FIGURE 1 Critical final concentrations needed to achieve 0.1% (*dotted line*), 1% (*solid line*), and 10% (*dashed line*) of the aqueous droplet in the oil that will have more than two enzyme molecules per emulsion droplet at various droplet diameters. In concentrations above the curves, >0.1%, 1%, or 10% of the droplets will have two or more enzyme molecules. The working concentration of 0.38 nM is drawn as the horizontal line. On average, each 1 $\mu$m diameter droplet will contain 0.12 molecules for the working concentration of 0.38 nM. This makes the observable enzyme reaction to be an all-or-nothing event.

droplet), 89% of all 1-$\mu$m-diameter droplets will contain no enzyme molecules, 10% will contain a single enzyme molecule, and ~1% will contain more than one molecule (see Fig. 2). Therefore, at this concentration, 90% of the 1-$\mu$m-droplets that show any presence of fluorescence contain a single enzyme molecule. Because only the droplets that contain the enzyme will be able to produce fluorescence, the droplets that do not contain enzyme will not be observable. As the diameter of the droplet decreases, the probability of the droplet containing more than one enzyme molecule also drops dramatically. This allows us to include the droplets with diameters <1 $\mu$m as part of the analysis.

The emulsion generation procedure that we used produces a heterogeneous distribution of droplet sizes (see Fig. 3). The background noise is ~15–20% of the mean background intensity after calibration, but the signal level for the droplets is much higher than the background noise. Although there are many spherical fluorescent droplets with a diameter <1 $\mu$m, there are also fluorescent droplets of larger sizes.

Positive control experiments using R110 fluorescent dye with no enzyme provide important results on two key issues, the uniformity of the emulsion (see Fig. 4, *A* and *B*) and the effect of photobleaching (see Fig. 4, *C* and *D*). Originally,

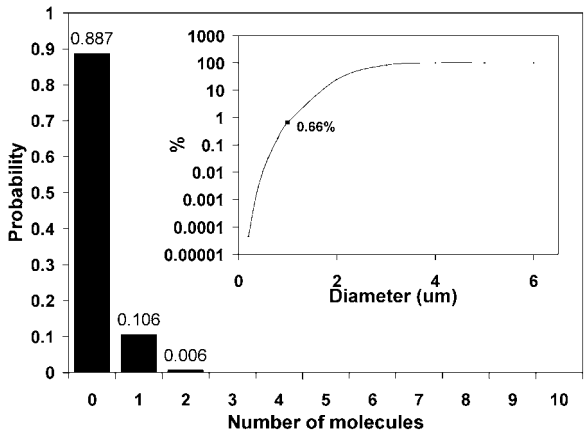


FIGURE 2 Poisson distribution for the working concentration of 0.38 nM in 1-$\mu$m droplet. Eighty-nine percent of the droplets have no molecules, 10% of the droplets have one molecule, <1% of the droplets have more than one molecule. The droplets that contain no enzyme molecule will not be observable under the fluorescence microscope. The inside figure shows the percentage of emulsion that will contain more than one enzyme molecule. At the working concentration of 0.38 nM, a droplet of 1 $\mu$m in diameter in the overall population will have 0.66% chance of containing more than one enzyme molecule.

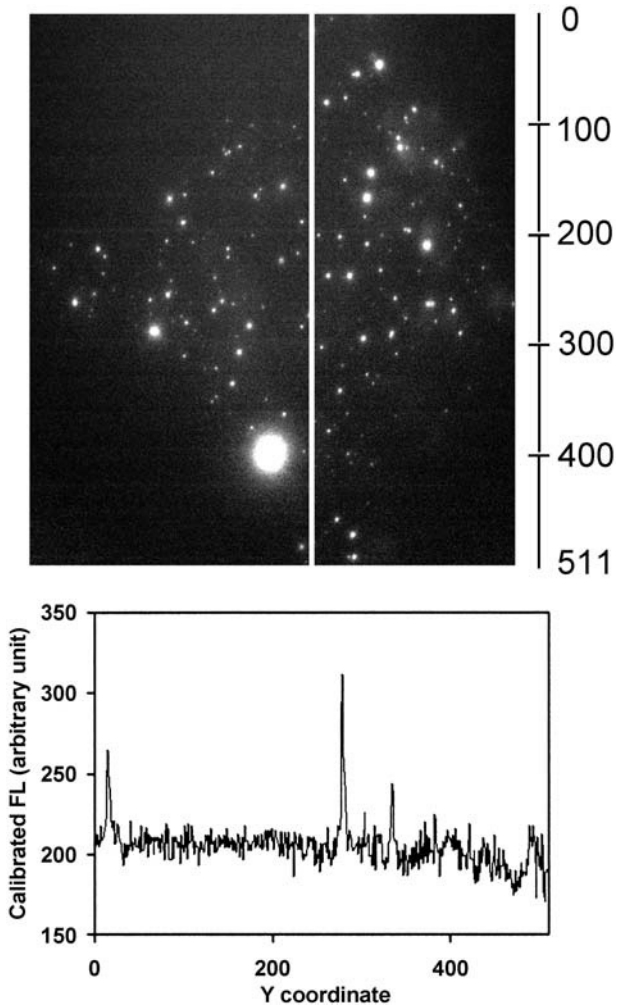


FIGURE 3 The positive control, with ~10 $\mu$M of R110 fluorophores but no enzyme in the droplets. The blender generates a range of different droplet sizes, but the majority of them are ~1 $\mu$m in diameter. Each droplet contains various amounts of fluorophore according to its size. At the bottom is the corrected fluorescence profile of the white line in the picture. The background noise is ~15–20% of the mean background intensity, but the signal level for the droplets is much higher than the background noise. This makes the background noise seem almost flat.

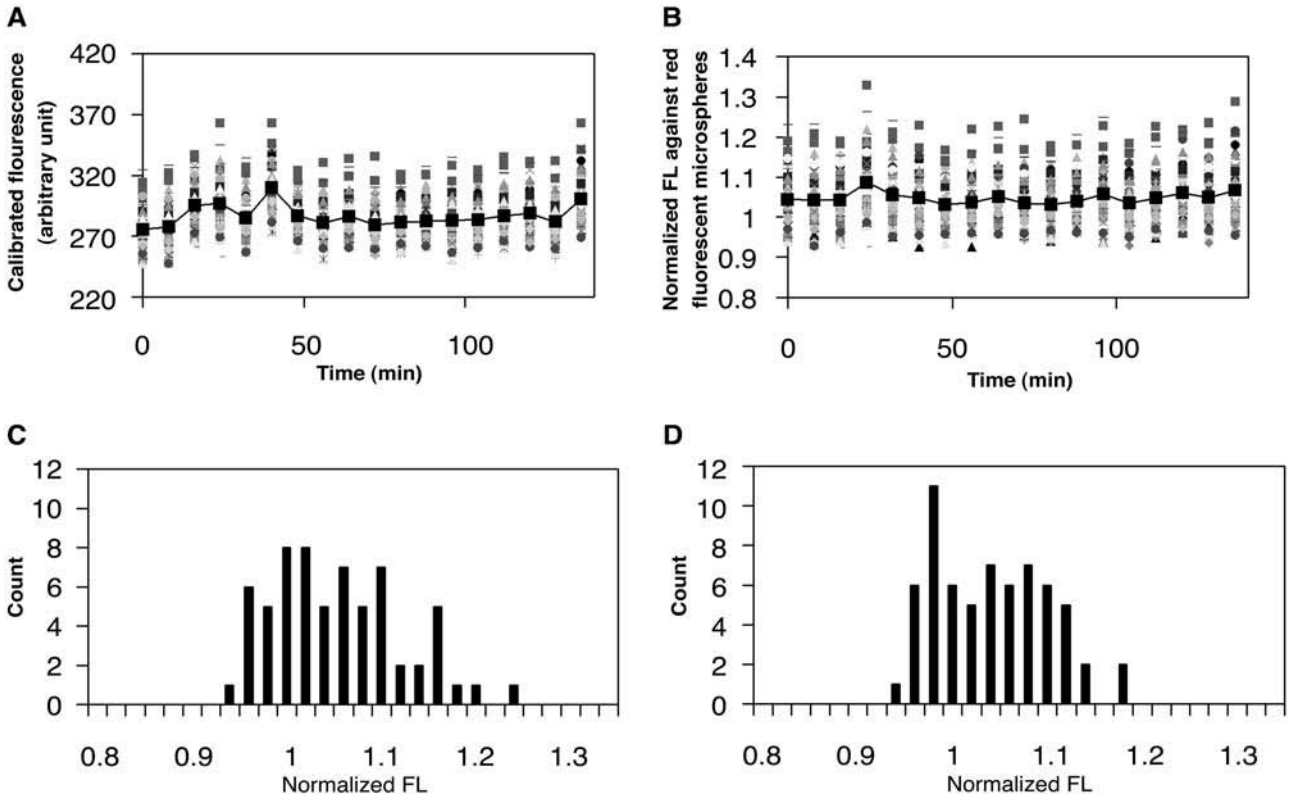


FIGURE 4 (*A* and *B*) Traces of the droplets in the positive control. There are 64 droplets that are tracked over a period of more than 2 h. (*A*) The raw fluorescence with a 10–12% variation and an overall standard deviation of 3.44%. The slope for the average is 0.0084. (*B*) The corrected fluorescence against the red fluorescence microspheres, with 5% variation and an overall standard deviation of 2.1%. The slope for the average is 0.00002. The average intensity of the droplets does not change dramatically with time after correction. (*C* and *D*) The distribution snapshots for control droplets at different times. (*C*) The distribution at 0 min. (*D*) The distribution at 80 min. As expected for the control experiment, there is no major shift in the mean ± SD of the distribution (1.044 ± 0.07 for 0 min and 1.032 ± 0.06 for 80 min).

the positive control droplets showed a variation in fluorescence intensity between 10% and 12% over time, with an average slope of 0.0084 (arbitrary intensity units/min). After the images are corrected with red fluorescent microsphere standards, the variation of fluorescence intensity in the positive control drops to 5% and the slope for the average also drops down to 0.00002 (arbitrary intensity units/min). The overall distribution also did not change over time, another indication of no reaction (1.044 ± 0.07 for 0 min and 1.032 ± 0.06 for 80 min). The decrease in the number of droplets in the high fluorescence region and the increase in the number of droplets in the low fluorescence region can both be attributed to photobleaching. The effect of photobleaching is not prominent under the experimental condition as indicated by the lack of change in the average intensity and distribution of intensity of the positive control droplets throughout the duration of the experiment. No fluorescence was detectable in negative control experiments using substrate only (data not shown), demonstrating that the fluorescence is a direct result of the chymotrypsin activity.

We can measure the activity of hundreds of individual droplets simultaneously (see Figs. 5 and 6). Measurements of fluorescence intensity, expressed as a percentage of the baseline, quantify the heterogeneity of the population (see Table 1). The fluorescence intensity increases with time (1.77% at 8 min and 6.36% at 80 min) as does the standard deviation of the distribution (3.69% at 8 min and 6.01% at 80 min), suggesting that the heterogeneity from each droplet is cumulative over time. The heterogeneity of the population of chymotrypsin can then also be quantified using histograms.

The overall coefficient of variation for the droplets is 6.7% at 0 min and 8.6% at 80 min (see Fig. 7). The distributions of droplets at both time points fit well in a Gaussian distribution, suggesting that the population under observation is fairly homogeneous. The coefficients of variation for the control experiment are fairly constant throughout the duration of the experiment (6.6% at 0 min and 5.8% at 80 min), suggesting that there is no change in the droplets. The experiment, on the other hand, showed a major increase in the coefficients of variation (4.8% at 0 min and 9.3% at 80 min), suggesting that droplets are acting differently from each other throughout the experiment (see Fig. 8). Although the activity of the population is heterogeneous, the percent increase in fluorescence for the individual measurements (0.058%/min) has a similar slope to that of the bulk measurements of chymotrypsin (0.076%/min) and the average percent increase for the indi-

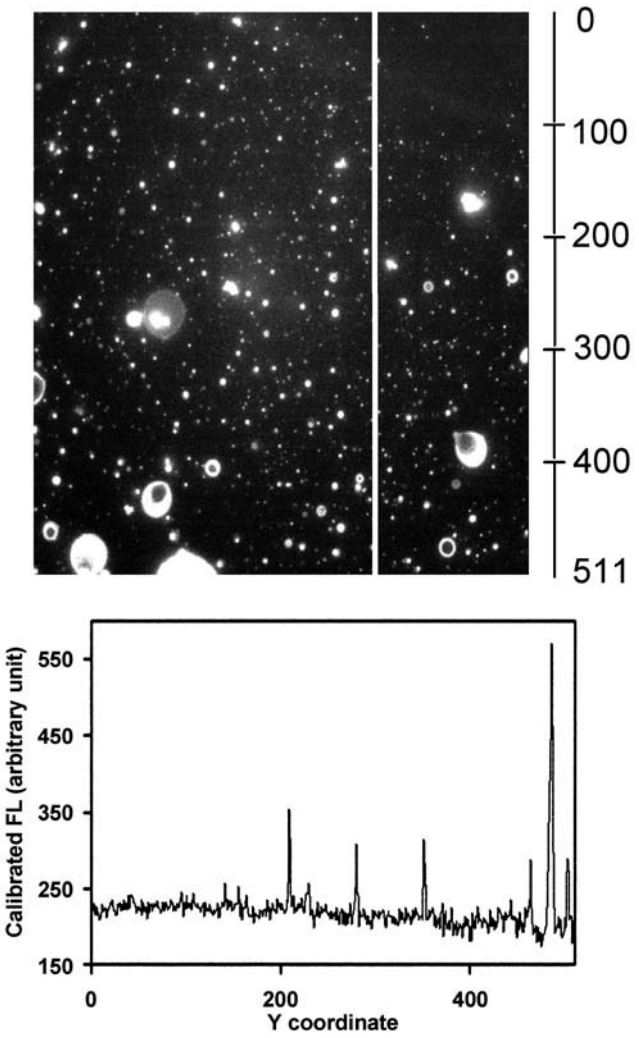


FIGURE 5 One of the time-lapse pictures during an experiment with enzyme and profluorescent substrate. The line profile shows the corrected fluorescence along the white line in the picture. For data analysis, we use only the droplets that are highly distinguishable from the background noise and present in all time-lapse pictures.

vidual mean is very close to the overall percent increase for the bulk measurements (6.35% for droplets and 6.03% for bulk) under similar conditions (see Fig. 9).

## DISCUSSION

We have developed an assay that can monitor the activity of hundreds of individual chymotrypsin molecules simultaneously. It should be applicable to other enzymes that have profluorescent substrates or have changes that can be observed optically. Furthermore, this assay can also be applied to any chemical reaction that can produce an optically detectable signal.

The ability to observe the activity of individual enzymes is based on the assumption that the distribution of enzymes

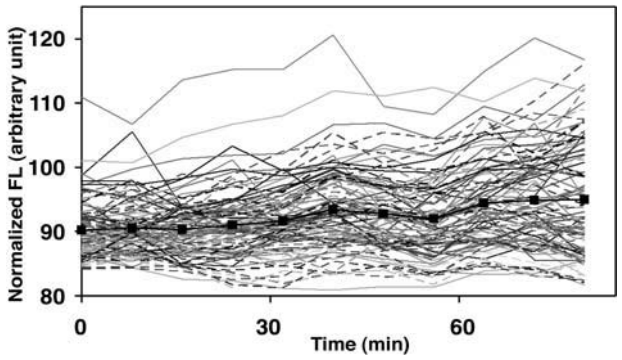


FIGURE 6 Kinetics of one particular experiment. In this set, there are 96 individual droplets traceable over time. Different traces showed different trajectories, with an overall increasing trend. The traces also demonstrated different reaction rates between different droplets. The emulsion assay can track multiple droplet data points simultaneously. The mean value of the individual traces is shown as the black line with square markers.

within droplets is random and follows a Poisson distribution. This assumption is valid if chymotrypsin does not interact with itself or with other molecules present. The use of the Poisson distribution to calculate the critical concentration needed for single-molecule experiments was mentioned by Greulich and has been explained in detail and validated by Földes-Papp and others (Földes-Papp et al., 2004; Greulich, 2004).

During the development of the assay, we noticed a 10–12% variation in the measured fluorescence intensity. Through control experiments, we established that this variation was intrinsic to the mercury lamp and microscope, attributing the latter to focus drift of the microscope objective. These variations impeded consistent results. To correct for this effect, we mixed 2.5-$\mu$m-diameter red fluorescent microspheres having a fluorescence spectrum similar to that of Texas Red into the oil phase, and used these microspheres as a reference. This allowed us to correct for most of the intrinsic variation of the imaging system and to pool results from different experimental runs together.

Despite careful alignment of the mercury lamp, we found a consistent 15–20% difference in illumination intensity across the field of view of the CCD camera. Although we corrected the overall levels of illumination using a flat field image, the most intense regions of illumination have higher

**TABLE 1 Mean ± SD of fluorescence intensity in experimental condition**

| | Time (min) | | | | | | | | | |
|---|---|---|---|---|---|---|---|---|---|---|
| | 8 | 16 | 24 | 32 | 40 | 48 | 56 | 64 | 72 | 80 |
| Mean (%) | 1.77 | 2.59 | 3.81 | 1.91 | 2.87 | 3.00 | 5.32 | 3.81 | 4.68 | 6.36 |
| SD (%) | 3.69 | 4.03 | 4.86 | 5.11 | 5.59 | 5.91 | 6.16 | 5.68 | 6.13 | 6.02 |

Measurements are expressed as the percent change relative to the intensity at 0 min, and show that fluorescence intensity in the experimental condition increases with time.

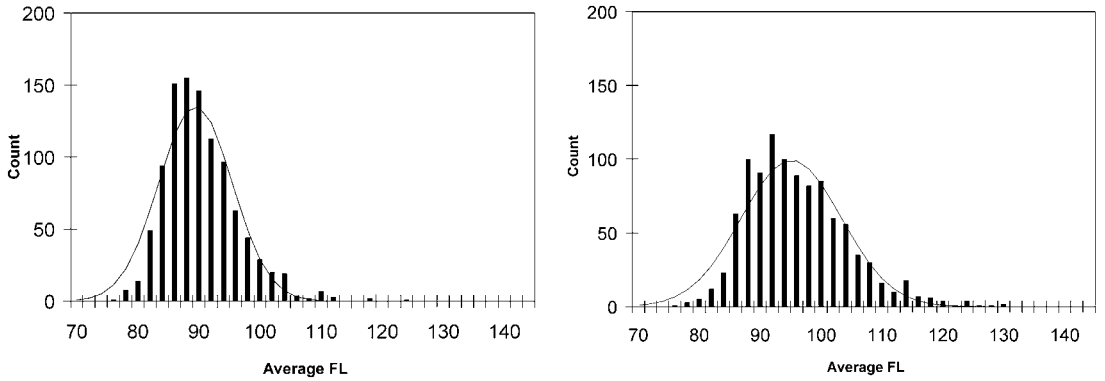


FIGURE 7 Distribution snapshots for pooled individual droplets (1023 in total) at different time points. The snapshot at left is the distribution at 0 min and the snapshot at right is the distribution at 80 min. Both distributions fit well under the Gaussian distribution indicated by the solid line. The distribution of the fluorescence from individual droplets showed a gradual shift of the population toward the right of the $x$ axis, showing that more substrate is cleaved by chymotrypsin. The mean is also shifted from 89.4 at 0 min to 95.1 at 80 min, a clear indication of the enzymatic reaction. The 0-min histogram has a coefficient of variation of 6.7% and the 80-min histogram has a coefficient of variation of 8.6%. This suggests that each droplet is reacting at its own reaction rate and accumulates a different amount of free fluorophore as time progresses.

background noise. This, in turn, causes difficulties in distinguishing between noise and actual signal in the center of the image, where the most intense illumination occurs. In cases like this, we simply excluded these data points from the analysis and focused on the signals in the surroundings.

By using R110 fluorophores only in the droplets as a control, we were able to ascertain the effectiveness of using a blender to create a uniform emulsion. As shown in Fig. 3, the blender generated a wide range of droplet sizes. We used image processing to select a fairly uniform-sized emulsion with a diameter of ~1 $\mu$m. The stringent criterion we set for the software is very good at filtering out droplets that are too big for consideration. When combined with the selection rule of position and presence in all time points, we recorded true droplets that served as individual reaction chambers. These rules allowed us to concentrate on the droplets that were 1 $\mu$m in diameter and below, where the chances of a droplet containing two or more enzyme molecules are low (<10% of the total observable population). However, these filtering rules do not allow us to filter out droplets that explicitly contain two or more enzyme molecules. The control also allows us to evaluate the role of photobleaching in the experiment. In Fig. 4 *B*, the fluorescence of the droplets in the

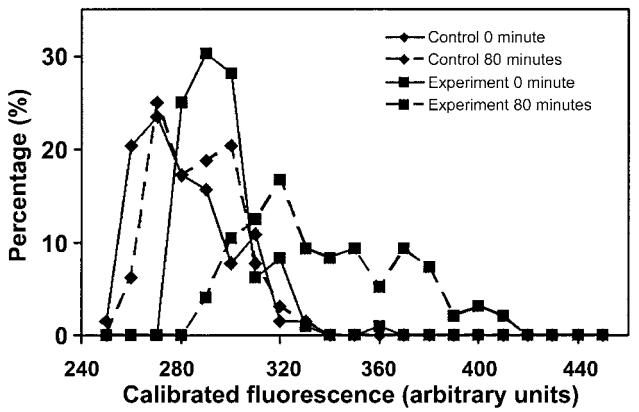


FIGURE 8 Comparison of the distribution pattern of fluorescence between control and experiments as time progresses. The diamond marked lines are the control experiment and the square marked lines are the experimental condition. The solid lines represent the time point at 0 min and the dashed lines represent the time point at 80 min. The control has a coefficient of variance of 6.6% for 0 min and 5.8% for 80 min. The experiment has a coefficient of variation of 4.8% for 0 min and 9.3% for 80 min. At 0 min, the control and the experimental both showed similar distributions, suggesting similar starting conditions. Later, at 80 min, the control still shows the same distribution spread, whereas the experimental distribution spread is almost doubled. This clearly indicates that there is an enzymatic reaction happening inside the droplets of the experimental condition.

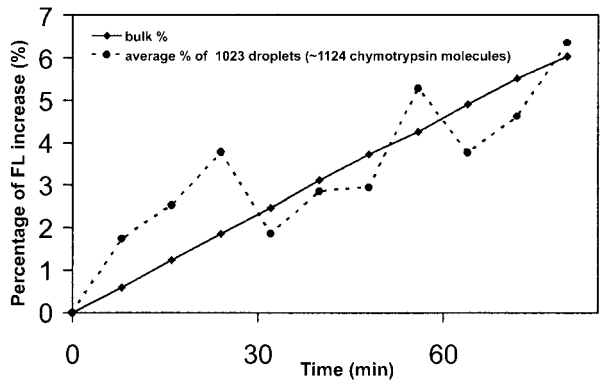


FIGURE 9 The kinetics comparison between a bulk population of chymotrypsin (*solid line*;~45.6 billion molecules, slope 0.076) and the average of individual droplets containing chymotrypsin pooled together (*dotted line*; 1023 droplets, ~1124 chymotrypsin molecules, slope 0.058). The trend of increase in the fluorescence intensity is very similar, as indicated by the similar overall percentage increase of fluorescence for both populations (6.03% for bulk and 6.35% for droplets). The average values from the individual droplets can be fitted against the values obtained from the ensemble average.

control experiment showed very little change when corrected against the variation of the optical system.

Photobleaching did not have a significant effect on our measurements. In the control experiments, we observed significant photobleaching of R110 only when the droplets were exposed to excitation light for 500 ms within short intervals (~30–60 s apart). Under normal experimental conditions, the control droplets showed very little decrease in fluorescence intensity, as indicated by the slope of the average line, which is 0.00002 (arbitrary intensity units/min) (Fig. 4 *B*). Each fluorophore can be excited a finite number of times before photobleaching. Photobleaching is one of the processes that the dye can undergo when it is excited. It is affected by a number of factors, including the number of excitation/emission cycles a dye molecule goes through and the surrounding environment (van den Engh and Farmer, 1992) This confirms the result where any fluctuation in the fluorescence after the correction against microscope variation is due to the chymotrypsin activity.

Although the overall trend of the fluorescence intensity increases for the individual droplets, the intensity occasionally drops. We can exclude photobleaching as a reason for this because we showed in the positive control that photobleaching is not significant. Two factors may contribute to the decrease in fluorescence intensity. First, changes in the focus of the microscope affect the recorded intensity. This problem can be corrected by the normalization against the fluorescent microspheres, because as the focus drifts, the fluorescence intensity from the microspheres also changes. Second, Brownian motion may cause changes in the position relative to the focal plane for these droplets.

When comparing the data obtained from the control and from the experiment, a significant difference develops as time progresses (Fig. 8). The control showed virtually no change in the distribution, whereas the distribution of the experiment spread out significantly. The control contained no enzyme. Therefore, the change in the distribution is due to the presence of enzyme. This observation confirms the presence of enzyme in the droplets and establishes the droplet as a suitable isolated reaction chamber.

The Poisson distribution provides a statistical description of the number of enzymes in the droplet. The distribution also exposes an artifact: some droplets will contain more than one enzyme. From the distribution, the ratio of droplets containing more than one enzyme to droplets containing one enzyme is ~1:10. In this work, we did not have the physical means to count the number of enzyme molecules inside a particular droplet. However, this could be done by labeling the enzyme with a different fluorophore.

The measured fluorescence increase for the bulk population is a manifestation of how chymotrypsin should behave on average, given this particular enzyme/substrate ratio (1:200,000). This bulk single-molecule comparison can be done graphically by converting the units on the *y* axis to the number of substrates cleaved per enzyme molecule for the bulk measurement. This allows us to estimate the number of droplets that contain two enzyme molecules in the visible droplet population.

The fraction of droplets containing more than one enzyme can be estimated from our data. The rate of the fluorescence produced by two enzyme molecules should be twice as large as that produced by a single enzyme, for a first-order reaction rate enzyme such as chymotrypsin. We consider the slope of the bulk population as a representation of an average single chymotrypsin molecule. We doubled the value of the slope, and used this as the cut-off value for our estimation for droplets that contain two molecules of chymotrypsin. We then calculated the slope for each individual droplet. We found that the number of droplets with a slope exceeding the cut-off value is ~10% of the total number of droplets screened (103 of 1023). This percentage agrees with the prediction from the Poisson distribution, suggesting that this method can provide a good estimate of the number of droplets that contain two enzyme molecules.

The processed kinetics data for individual chymotrypsin molecules reveal several interesting features (Figs. 6 and 7). First, the increase in the fluorescence intensity shows that the enzyme activity is indeed present and the change is significant enough to be detectable. This suggests that the emulsion system is capable of running isolated chemical reactions. The individual droplets can be considered as reaction chambers where the reaction environments are isolated from each other.

Second, the mean measured activity of individual droplets (1023 droplets, ~1124 molecules total) is similar to that of a bulk population (~45.6 billion molecules) of chymotrypsin (Fig. 9). It is possible to analyze the kinetics of a reaction using a very small amount of material. The individual trace over time for each droplet is not a smooth line, suggesting that the enzyme does not function at a constant rate. Rather, there may be some period of time where the enzyme slowed down or sped up. This is similar to the ''memory'' effect for enzymes described by Edman and others and Qian and others (Edman and Rigler, 2000; Qian and Elson, 2002). This kind of phenomenon will be hidden in the bulk population data, but revealed in the single-molecule measurements.

Finally, the individual droplet data can be converted into a distribution snapshot at various time points that shows the range of activity encompassed by the individual molecules (Fig. 7). The snapshots clearly show that as time progresses, the distribution of the enzyme activity becomes wider (Table 1). Most of the chymotrypsin molecules have a rate within a narrow range, yet other molecules have higher or lower rates compared to the normal population. The enzymes are neither acting at a constant rate nor acting synchronously.

Our results are similar to those obtained using other techniques and other enzymes. Dyck and Craig employed capillary electrophoresis as the medium for single-molecule enzyme isolation. Using this method, they were able to produce a population distribution on the activity of alkaline

phosphatase. The distribution histogram clearly shows the heterogeneity of the enzyme (Dyck and Craig, 2002). Werner and others found that exonuclease I displays population heterogeneity in the rate of cleaving DNA bases by immobilizing a strand of synthesized DNA with two fluorescently labeled bases separated by a known distance and observing the activity of exonuclease I as it cleaves off the bases of the DNA (Werner et al., 2005). Rueda and others employed fluorescence resonance energy transfer (FRET) on immobilized ribozymes to detect the docking and undocking constants for its substrate. Part of their result shows that the constants they derived from single-molecule FRET are consistent with the constants they derived from bulk FRET averages. The same result was also observed by Greulich, where the Michaelis-Menten constant for a single lactate dehydrogenase falls within the range of the constant from the bulk population (Greulich, 2004; Rueda et al., 2004). These results agree with our observations.

## CONCLUSION

With this emulsion assay, we can measure multiple single-molecule enzymatic reactions simultaneously. Based on the results, we conclude that enzyme activity is present and measurable in micron-diameter water-in-oil droplets. The results clearly showed the heterogeneity of chymotrypsin activity and demonstrated the individuality of each molecule. The assay also allows the measurement of enzyme kinetics with very few molecules and provides results consistent with the bulk population. The measurements of the activity of individual enzymes can be averaged to obtain results similar to measurements made in bulk. This ability to gather multiple single-molecule data points is key for studying enzyme-inhibitor interactions, when the enzyme kinetics cannot be analyzed using the classic Michaelis-Menten model due to cooperativity or other factors.

Several technical innovations could lead to improvements in this system. Clearly, a system that can create an emulsion with uniform droplet sizes would simplify the data analysis. An emulsion generation system that has the ability to generate many individual droplets rapidly is under development (Tan et al., 2003). With a more sophisticated droplet generation method to ensure the uniformity of the droplet size, we can control the variation within the droplets further and allow for more precise control over the single-molecule environment. With the possibility of advanced microfluidic control, there is also the potential of using the droplet environment to create assays that involve multiple reagents. This new assay provides the ability to monitor large numbers of individual molecules simultaneously, allowing efficient large-scale screening of chemical reactions. The single-molecule detection concept also allows analysis of a limited amount of material. This assay is also compatible with large-scale microfluidic implementations of a lab-on-a-chip.

This work was supported by National Science Foundation grant CCR-0304612.

## REFERENCES

Allen, S., S. M. Rigby-Singleton, H. Harris, M. C. Davies, and P. O'Shea. 2003. Measuring and visualizing single molecular interactions in biology. *Biochem. Soc. Trans.* 31:1052–1057.

Dyck, A. C., and D. B. Craig. 2002. Individual molecules of thermostable alkaline phosphatase support different catalytic rates at room temperature. *Luminescence.* 17:15–18.

Edman, L., Z. Földes-Papp, S. Wennmalm, and R. Rigler. 1999. The fluctuating enzyme: a single molecule approach. *Chem. Phys.* 247:11–22.

Edman, L., and R. Rigler. 2000. Memory landscapes of single-enzyme molecules. *Proc. Natl. Acad. Sci. USA.* 97:8266–8271.

Edwardson, J. M., and R. M. Henderson. 2004. Atomic force microscopy and drug discovery. *Drug Discov. Today.* 9:64–71.

Engler, N., A. Ostermann, N. Niimura, and F. G. Parak. 2003. Hydrogen atoms in proteins: positions and dynamics. *Proc. Natl. Acad. Sci. USA.* 100:10243–10248.

Földes-Papp, Z., U. Demel, and G. P. Tilz. 2004. A new concept for ultrasensitive fluorescence measurements of molecules in solution and membrane: 1. Theory and a first application. *J. Immunol. Methods.* 286:1–11.

Frauenfelder, H., B. H. McMahon, and P. W. Fenimore. 2003. Myoglobin: the hydrogen atom of biology and a paradigm of complexity. *Proc. Natl. Acad. Sci. USA.* 100:8615–8617.

Greulich, K. O. 2004. Single molecule techniques for biomedicine and pharmacology. *Curr. Pharm. Biotechnol.* 5:243–259.

Ha, T. 2001. Single-molecule fluorescence resonance energy transfer. *Methods.* 25:78–86.

Hinterdorfer, P., G. Schutz, F. Kienberger, and H. Schindler. 2001. Detection and characterization of single biomolecules at surfaces. *J. Biotechnol.* 82:25–35.

Ishii, Y., K. Kitamura, H. Tanaka, and T. Yanagida. 2003. Molecular motors and single-molecule enzymology. *Methods Enzymol.* 361:228–245.

Ishii, Y., and T. Yanagida. 2000. Single molecule detection in life science. *Single Molecule.* 1:5–16.

Ishijima, A., T. Doi, K. Sakurada, and T. Yanagida. 1991. Sub-piconewton force fluctuations of actomyosin in vitro. *Nature.* 352:301–306.

Ishijima, A., and T. Yanagida. 2001. Single molecule nanobioscience. *Trends Biochem. Sci.* 26:438–444.

Jares-Erijman, E. A., and T. M. Jovin. 2003. FRET imaging. *Nat. Biotechnol.* 21:1387–1395.

Kulzer, F., and M. Orrit. 2004. Single-molecule optics. *Annu. Rev. Phys. Chem.* 55:585–611.

Liem, L. K., J. M. Simard, Y. Song, and K. Tewari. 1995. The patch clamp technique. *Neurosurgery.* 36:382–392.

Lu, H. P., L. Xun, and X. S. Xie. 1998. Single-molecule enzymatic dynamics. *Science.* 282:1877–1882.

Medina, M. A., and P. Schwille. 2002. Fluorescence correlation spectroscopy for the detection and study of single molecules in biology. *Bioessays.* 24:758–764.

Muller, D. J., H. Janovjak, T. Lehto, L. Kuerschner, and K. Anderson. 2002. Observing structure, function and assembly of single proteins by AFM. *Prog. Biophys. Mol. Biol.* 79:1–43.

Nie, S., and R. N. Zare. 1997. Optical detection of single molecules. *Annu. Rev. Biophys. Biomol. Struct.* 26:567–596.

Noji, H., R. Yasuda, M. Yoshida, and K. Kinosita, Jr. 1997. Direct observation of the rotation of F1-ATPase. *Nature.* 386:299–302.

Park, M. K., A. V. Tepikin, and O. H. Petersen. 2002. What can we learn about cell signalling by combining optical imaging and patch clamp techniques? *Pflugers Arch.* 444:305–316.

Qian, H., and E. L. Elson. 2002. Single-molecule enzymology: stochastic Michaelis-Menten kinetics. *Biophys. Chem.* 101–102:565–576.

Rueda, D., G. Bokinsky, M. M. Rhodes, M. J. Rust, X. Zhuang, and N. G. Walter. 2004. Single-molecule enzymology of RNA: Essential functional groups impact catalysis from a distance. *Proc. Natl. Acad. Sci. USA.* 101: 10066–10071.

Sakmann, B., and E. Neher. 1984. Patch clamp techniques for studying ionic channels in excitable membranes. *Annu. Rev. Physiol.* 46:455–472.

Tan, Y. C., J. Collins, and A. P. Lee. 2003. Nanojet controlled droplet emulsion in microfluidic channels. *Proc. MicroTAS Conference*, Squaw Valley, CA. 963–966.

van den Engh, G., and C. Farmer. 1992. Photo-bleaching and photon saturation in flow cytometry. *Cytometry.* 13:669–677.

Weiss, S. 1999. Fluorescence spectroscopy of single biomolecules. *Science.* 283:1676–1683.

Weiss, S. 2000. Measuring conformational dynamics of biomolecules by single molecule fluorescence spectroscopy. *Nat. Struct. Biol.* 7:724–729.

Werner, J. H., H. Cai, R. A. Keller, and P. M. Goodwin. 2005. Exonuclease I hydrolyzes DNA with a distribution of rates. *Biophys. J.* 88:1403–1412.

Whitesides, G. M., E. Ostuni, S. Takayama, X. Jiang, and D. E. Ingber. 2001. Soft lithography in biology and biochemistry. *Annu. Rev. Biomed. Eng.* 3:335–373.

Xie, X. S., and H. P. Lu. 1999. Single-molecule enzymology. *J. Biol. Chem.* 274:15967–15970.

Xie, X. S., and J. K. Trautman. 1998. Optical studies of single molecules at room temperature. *Annu. Rev. Phys. Chem.* 49:441–480.

Yang, H., G. Luo, P. Karnchanaphanurach, T. M. Louie, I. Rech, S. Cova, L. Xun, and X. S. Xie. 2003. Protein conformational dynamics probed by single-molecule electron transfer. *Science.* 302:262–266.